Changing Yarn Hairiness During Winding— Analyzing the Trailing Fiber Ends

Jun Lang, Sukang Zhu and Ning Pan

Textile Research Journal 2004; 74; 905
DOI: 10.1177/004051750407401010

Changing Yarn Hairiness During Winding—Analyzing the Trailing Fiber Ends

JUN LANG AND SUKANG ZHU[1]

Center of Physics of Fibrous Materials, Dong Hua University, Shanghai 200051, People's Republic of China

NING PAN

Division of Textiles and Clothing, Biological and Agricultural Engineering Department, University of California, Davis, California 95616, U.S.A.

ABSTRACT

The change mechanisms of staple yarn hairiness during the winding process are studied using some previously published theories on yarn structures. Of the three kinds of yarn hairiness, the one formed by trailing and protruding fiber ends is analyzed first in terms of the interactions of the fiber ends, the tension disk, and the grooved drum. The various actions on the yarn during the winding process are identified and categorized into two groups: the one pulling the fiber ends and the other providing the resistance. By defining a ratio of the two groups of forces, a criterion of whether a fiber can be pulled out is established. This criterion is then applied to the tension disk and grooved drum, the main sites where actions occur, to investigate the impact on yarn hairiness. The influences of some important parameters including the yarn twist factor, the embedded fiber length, the frictional coefficients, and the size of the cheese are examined.

Barella [1] classified yarn hairiness into three types: protruding fiber ends, fiber loops, and wild fibers. For ring-spun yarns, Wang [25] pointed out that yarn hairiness may consist of 82–87% protruding fiber ends (including both leading and trailing ends), 9–12% fiber loops, and 4–6% wild fibers. Previous researchers [4, 8, 10, 18, 26, 27] focused mainly on the influence of fiber properties (length, diameter, rigidity) and spinning conditions on yarn hairiness, as well as the measurements and measuring equipment for hairiness.

Rust and Peykamian [21] revealed that fibers migrate even during the winding process, increasing yarn hairiness afterwards, and a higher winding tension and/or higher yarn velocity leads to more fiber migration and hence more severe yarn hairiness. Tarafder [23] studied the influence of the winding process on yarn hairiness; he observed that the increased hairiness at the bottom of the bobbin was greater than that at the top after winding. Chellamani [3] and Krishnaswamy [7] found that the number of short fiber trailing ends decreased due to winding if the bobbin yarn was excessively hairy.

During the winding process, when a yarn passes the tension disk, the yarn guide, and the grooved drum, the loose fiber ends on the surface of the yarn are rubbed acutely, which inevitably causes changes in yarn hairiness. However, the details or the physical mechanisms of such changes have been virtually overlooked, and there are no theoretical analyses of this issue in previously published studies. In this paper, we mainly explore the problem of yarn hairiness changes due to contact with the tension disk and grooved drum during the winding process. Because most of the hairiness is of the protruding fiber end type, we will focus on protruding hairiness, and more specifically, on trailing hairiness.

Interactions of Trailing Fiber Ends and Tension Disk

When a protruding fiber end is in contact with the tension disk during the winding process, the contacting model is as illustrated in Figure 1, where L_g is the width of the tension disk, L_{fr} is the length of the trailing fiber end, T_0 and T_1 are the initial and exit yarn tensions, V is the velocity of the yarn, and a, b are the end surfaces of the tension disk. Further, as shown in Figure 1, the embedded part of the fiber in the yarn can either be in the same direction as yarn hairiness (dashed line) or in the reverse direction (solid line). We call the former the leading protruding fiber hair and the latter the trailing protruding fiber hair.

[1] Corresponding author: zusukang@dhu.edu.cn

  0040-5175/$15.00

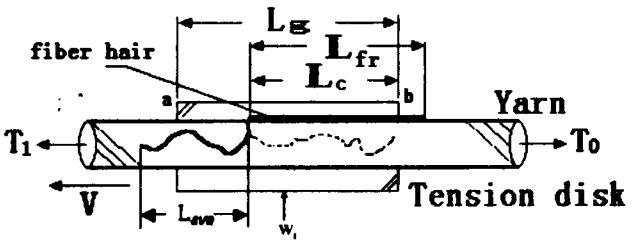

FIGURE 1. Friction between the tension disk and a fiber hair.

When a yarn passes the tension disk, a simple force analysis shows that there are different actions such as the gripping force P of the yarn acting on the embedded length of the fiber, the pulling force F_1 exerted by the tension disk on the fiber hair due to friction, and the resistance F_2 on the hair by yarn surface friction, as shown in Figure 2a. If we select a cross section of the yarn in Figure 2b, the pressure per unit length acted by the tension disk on the yarn is W_p.

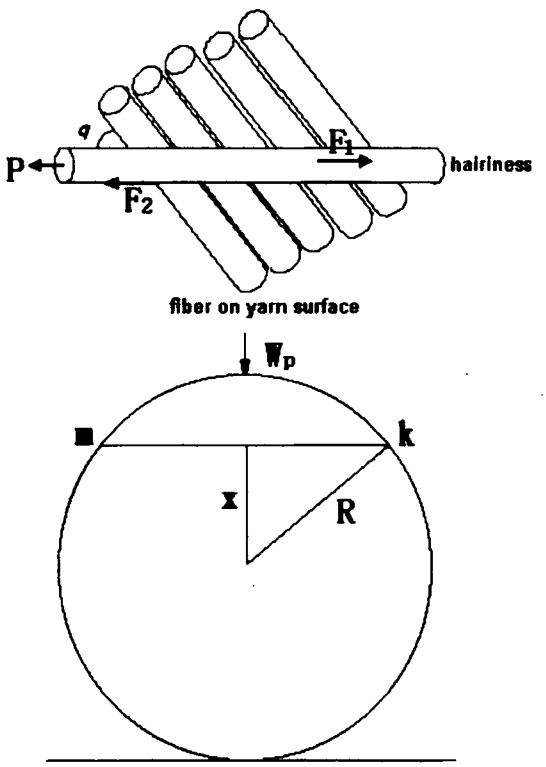

FIGURE 2. (a) Force balance on the yarn, (b) cross section of the yarn.

As in most analyses, we assume that all fibers have a cylindrical shape and are identical in physical and geometric properties.

MEAN GRIPPING FORCE ON AN EMBEDDED FIBER LENGTH

Usually when the yarn twist level is mildly high or the yarn tension is small, the slippage of fibers during yarn extension can be neglected as demonstrated by Platt [20]. Platt examined the load-elongation relationship of staple yarns that have the same fiber length but a different twist level; the results are shown in Figures 3a and b for two cases of fiber length at 2.5 inches (63.5 mm) and 1.5 inches (38.1 mm), respectively.

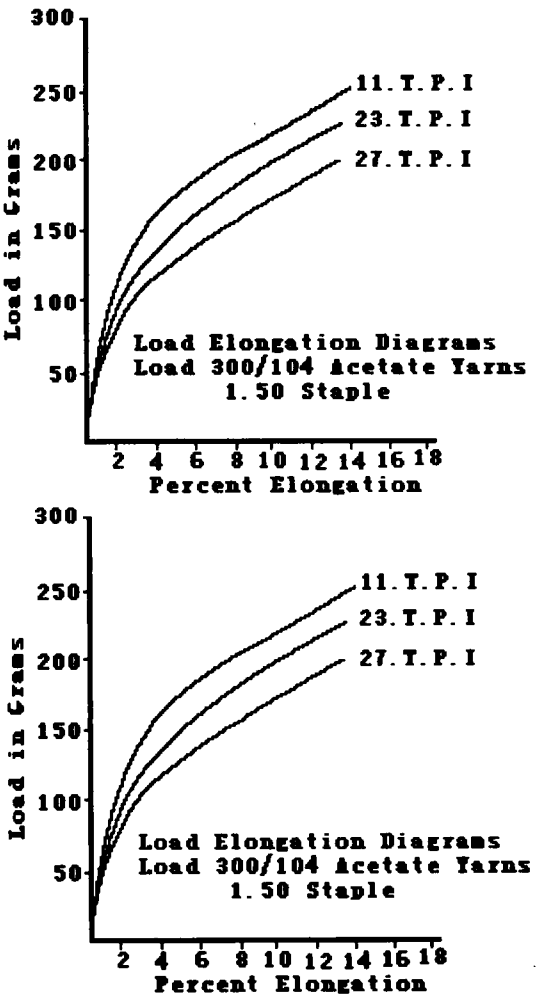

FIGURE 3. (a) Acetate yarns (2.5 in.) load-elongation curve [20], (b) acetate yarns (1.5 in.) load-elongation curve [20].

In each figure, when tension in the yarn is relatively large, the elongation differences of the yarns caused by both stress transfer between fibers and fiber slippage during yarn extension [11, 12] at three different twist levels become significant. Additionally, comparing the results at the same load level reveals that the discrepancy

is more apparent in shorter fiber cases. In the winding process, the yarn tension is considerably smaller than the yarn-breaking load; the slippage of the fibers can hence be neglected for simplicity.

The embedded part L_e of a fiber is gripped by neighboring fibers in the yarn mainly by frictional force, which is determined by the pressure on the embedded length:

$$G = g_\lambda + g_w \quad , \tag{1}$$

where g_w is the transverse pressure from the tension disk and g_λ is the internal yarn lateral pressure determined by the yarn structure.

According to the analysis in references 11, 12, 16, and 17, when a yarn is in tension T, the mean lateral pressure g exerted on the embedded fiber length can be derived as

$$g = \frac{v}{2\mu_1} E_f \frac{T}{\pi n_1 \bar{r}_f^2 E_L} \eta_q \tanh(vs_e) \quad , \tag{2a}$$

where E_f is the fiber modulus, μ_1 is the frictional coefficient between the embedded and the neighboring fibers, $s_e = \frac{L_e}{2r_f}$ is the embedded aspect ratio of the fiber, and v is the cohesion factor, an indicator of the gripping effect of the yarn structure on each individual fiber, and can be calculated according to Pan [11]. The longitudinal tensile modulus of the yarn E_L, the mean number of the fibers in the yarn cross section n_1, the mean radius of the cut fiber ends in the yarn cross section $\bar{r}_f$, and the so-called fiber orientation efficiency factor η_q can all be calculated from references 11, 16, and 17; all are functions of the helix angle q of the fiber on the yarn surface or the yarn twist factor T_y.

One important assumption in Pan's theory is that fibers contact each other closely over the fiber length. But in reality, this is usually not the case because of the discrete nature of fiber contact. So Equation 2a should be modified as

$$g_\lambda = \lambda \frac{v}{2\mu_1} E_f \frac{T}{\pi n_1 \bar{r}_f^2 E_L} \eta_q \tanh(vs_e) \quad , \tag{2b}$$

where λ is a correction factor whose value can be calculated as

$$\lambda = n_e \frac{D_f}{L_e} \quad , \tag{2c}$$

where D_f is the fiber diameter, and n_e is the mean number of the contacting fibers over the length L_e. For a twisted yarn, n_e can be calculated from reference 15.

The pressure g_w on a fiber from the tension disk is not a constant because of fiber migration. If we select a cross section of the yarn (see Figure 2b), and the pressure per unit length acted by the tension disk against the yarn is W_p, the mean compressive stress $\bar{W}$ over the line L_{mk} can be derived as

$$\bar{W} = \frac{W_p}{L_{mk}} = \frac{W_p}{2\sqrt{R^2 - x^2}} \quad , \tag{3a}$$

where R is the radius of the yarn, and can be derived as

$$R = \sqrt{\frac{n_1}{V_f}} \cdot \bar{r}_f \quad , \tag{3b}$$

where V_f is the fiber volume fraction defined and calculated in reference 11.

The mean transverse pressure over the whole yarn cross section will be

$$g_w = \frac{1}{R}\int_0^R \bar{W} dx = \frac{\int_0^R \frac{W_p}{\sqrt{R^2 - x^2}} dx}{2R}$$

$$= \frac{W_p \pi}{4R} = \frac{W_p \pi}{4r_f} \sqrt{\frac{1 + \cos q}{2}} \sqrt{V_f} \quad . \tag{3c}$$

Thus for a given yarn tension T, the mean gripping force P on the embedded part of the hairy fiber can be calculated as

$$P = P_1 + P_2 = g_\lambda \mu_1 2\pi r_f L_e + g_w \mu_1 2\pi r_f L_e$$

$$= T f_1(T_y, S_e) + W_p \mu_1 f_2(T_y, S_e) \quad , \tag{4a}$$

where

$$f_1(T_y, S_e) = 2v\eta_q \frac{n_e}{n_1} \frac{E_f}{E_l} \tanh(vS_e) \tag{4b}$$

and

$$f_2(T_y, S_e) = \frac{L_e \pi^2}{2} \sqrt{\frac{1 + \cos q}{2}} \sqrt{V_f} \quad . \tag{4c}$$

So it is clear from Equation 4 that the total gripping force is related to both the intrinsic characteristics T_y and S_e of the yarn and the winding parameters T and W_p.

Friction Between a Fiber Hair and the Yarn Surface

A simple illustration of a trailing fiber end contacting the yarn surface is shown in Figure 2a, and this case is similar to the one analyzed by Pan [13, 14], which we have adopted here. Because the fiber end is pressed by only mild force during winding, the deformation of the fiber itself can be neglected. When the fiber end has a tendency to move due to friction from the tension disk,

the resistance from a single fiber contacting point, which is caused by friction with the yarn surface, is [13, 14]

$$F_i = \frac{\tau_s D_f^2/\sin q}{\beta} \tanh(\beta) \quad , \tag{5a}$$

where τ_s is the nominal shear strength per unit area, and β is a parameter defined and calculated in references 13, 14. If the length of the trailing end contacting the yarn surface is L_c, the total number of contacting points is

$$n_2 = \text{int}\left(\frac{L_c \sin q}{D_f}\right) \quad . \tag{5b}$$

Thus the total resistance to fiber hair movement relative to the yarn surface is

$$F_2 = \sum_{i=1}^{n_2} F_i = \text{int}\left(\frac{L_c \sin q}{D_f}\right) \frac{\tau_s D_f^2/\sin q}{\beta} \tanh(\beta) \quad . \tag{5c}$$

From Figure 2a, we know the nominal contacting area of the fiber hair with the yarn surface:

$$A_c = \text{int}\left(\frac{L_c \sin q}{D_f}\right) \frac{D_f^2}{\sin q} \quad . \tag{6a}$$

The whole shear force on the contacting area τ_{total} should be

$$\tau_{\text{total}} = A_c \tau_s = \text{int}\left(\frac{L_c \sin q}{D_f}\right) \frac{D_f^2}{\sin q} \tau_s \quad . \tag{6b}$$

In fact, because this shear force is provided by the frictional force between the fiber end and the yarn surface (neglecting adhesion), it should be related to the compressive force W as

$$\tau_{\text{total}} = \mu_1 W \quad . \tag{6c}$$

Substituting these results into 5c, the total resistance caused by the yarn surface is

$$F_2 = \frac{W\mu_1}{\beta} \tanh(\beta) = \tau_{\text{total}} \frac{\tanh(\beta)}{\beta} \quad . \tag{7}$$

From Equation 7, it is clear that the total resistance is not equal to the nominal frictional force between the yarn surface and the fiber end. The ratio $\frac{\tanh(\beta)}{\beta}$ is a very interesting parameter representing the yarn structural properties and twisting effect as discussed in references 11, 12, 13, and 14. Note that $\frac{\tanh(\beta)}{\beta} \to 1$ when $\beta \to 0$ and $\frac{\tanh(\beta)}{\beta} \to 0$ when $\beta \to \infty$. So it is apparent that the actual frictional force F_2 is smaller than the value calculated using Amonton's law due to the topological features of the yarn and will further decrease when the twist increases.

Frictional Force Between Fiber End and Tension Disk

When the total compression force on the tension disk W_t is given, the compression force W between the fiber end and the tension disk, as shown in Figure 1, can be obtained as

$$W = \frac{W_t}{L_g} L_c \quad , \tag{8}$$

where L_g is the width of the tension disk. The frictional force between the fiber end and the tension disk then follows:

$$F_1 = \frac{L_c}{L_g} W_t \mu_2 \quad . \tag{9}$$

Calculations and Discussion

Effects of the Tension Disk

According to Figure 1, when the yarn passes the tension disk from b to a, the tension of the yarn changes from T_0 to T_1. Because the yarn is virtually straight during movement, we consider this tension change to be linear. Further, if point b is taken as the origin of the X coordinate, the tension T versus X is shown in Figure 4. Denoting the net length of the yarn as $X_2 - X_1$, the mean tension on the yarn can then be expressed by the tension at the position of $(X_2 + X_1)/2$. Next, we define a dimensionless parameter,

$$K = \frac{F_1 - F_2}{P} \quad . \tag{10}$$

Obviously, the necessary and sufficient condition for a fiber being pulled out is $F_1 > F_2 + P$ or $K > 1$.

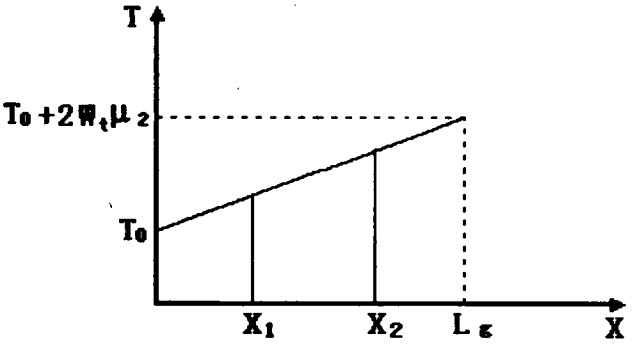

FIGURE 4. Yarn tension change through the tension disk.

According to Figure 1, if the fiber length is L_f, the length of the embedded part is $L_e = L_f - L_{fr}$. Then the mean projected length L_{ave} of the embedded fiber length in Figure 1 in the direction of the yarn axis is

$$L_{ave} = \frac{\int_0^q L_e \cos\theta d\theta}{q} = \frac{L_e \sin q}{q} \quad . \tag{11}$$

For the trailing fiber end, the frictional force from the tension disk can be calculated from Equation 9. After substituting Equation 8 into 7, the frictional resistance by the yarn surface can be derived as well:

$$F_2 = W_t \mu_1 \frac{L_c}{L_g} \frac{\tanh \beta}{\beta} \quad . \tag{12a}$$

The pull-out force F_p, which is the difference between F_1 and F_2, is

$$F_p = F_1 - F_2 = W_t \mu_2 \frac{L_c}{L_g} \left(1 - \frac{\mu_1}{\mu_2} \frac{\tanh \beta}{\beta}\right) \quad , \tag{12b}$$

so the necessary condition for a fiber hair to be pulled out is $F_p > 0$, or

$$\frac{\tanh \beta}{\beta} < \frac{\mu_2}{\mu_1} \tag{13a}$$

or

$$\mu_2 > \mu_1 \quad . \tag{13b}$$

In the initial moment of the bobbin unwinding process, the yarn tension is very small and can be taken as zero. The mean tension T_{ave} of the yarn segment, which includes the embedded part of the fiber hair, is

$$T_{ave} = \left(\frac{L_c + L_{ave}}{L_g} + \frac{L_c}{L_g}\right) W_t \mu_2 = (2L_c + L_{ave}) \frac{W_t \mu_2}{L_g} \quad . \tag{14a}$$

Plugging Equations 7 and 27 into 11, we get the gripping force of the yarn on the embedded fiber length:

$$P = \frac{W_t \mu_2}{L_g} (2L_c + L_{ave}) \cdot f_1(T_y, S_e) + \frac{W_t \mu_1}{L_g} \cdot f_2(T_y, S_e) \quad . \tag{14b}$$

Equation 10 can then be rewritten as

$$K = \frac{\alpha_1 L_c}{\alpha_2 L_c + \gamma_2} \quad , \tag{15a}$$

where

$$\alpha_1 = 1 - \frac{\mu_1}{\mu_2} \frac{\tanh \beta}{\beta} \quad , \tag{15b}$$

$$\alpha_2 = 2f_1(T_y, S_e) \quad , \tag{15c}$$

$$\gamma_2 = f_1(T_y, S_e) L_{ave} + \frac{\mu_1}{\mu_2} f_2(T_y, S_e) \quad . \tag{15d}$$

From Equation 15a, the value of K is independent of the pressure from the tension disk. When the embedded fiber aspect ratio S_e is constant, α_1 can represent the change rate of the hair pulling-out force, whereas α_2 reflects the change rate of the gripping force on the contacting length, and γ_2 can represent the gripping force related only to yarn structure and the length of the hair engaged in the tension disk.

When the hair contact length L_c is below a certain value, K is small so the fiber cannot be pulled out from the yarn. (The fiber can, and often does, break inside the yarn, but this will not increase the hairiness and therefore will not affect our discussion.) So in general, a larger K value leads to the greater possibility of the fiber being pulled out. Differentiating Equation 15a yields

$$\frac{dK}{dL_c} = \frac{\alpha_1 \gamma_2}{(\alpha_2 X + \gamma_2)^2} \quad . \tag{16}$$

If the product of α_1 and γ_2 is positive, the value of K will increase with the value of L_c. From Equations 5 and 15d, γ_2 must be greater than zero. In Equation 15b, for the fiber to be pulled out, there must be $\frac{\mu_1}{\mu_2} \frac{\tanh \beta}{\beta} < 1$ or $\alpha_1 > 0$. Furthermore, by plotting α_1 and α_2 against the twist factor T_y in Figures 5 and 6, using the data in Table I, we learn from the figures that when the embedded length or S_e of a fiber is constant, the value of α_1, and

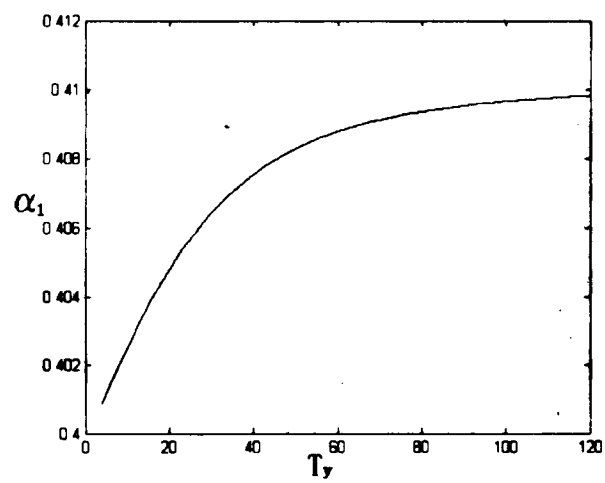

FIGURE 5. Relationship between α_1 and twist factor T_y.

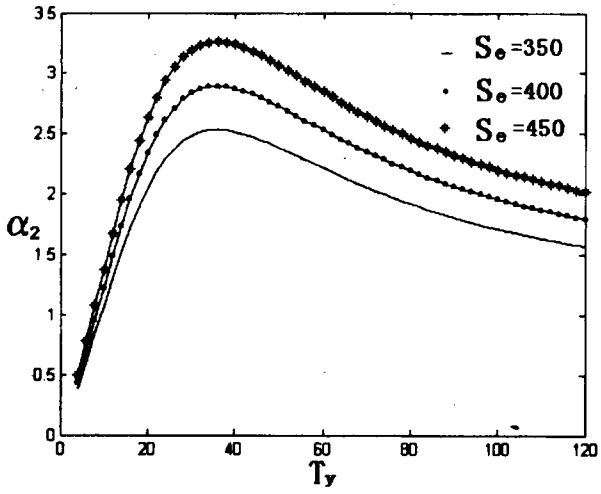

FIGURE 6. Relationship between α_2 and twist factor T_y.

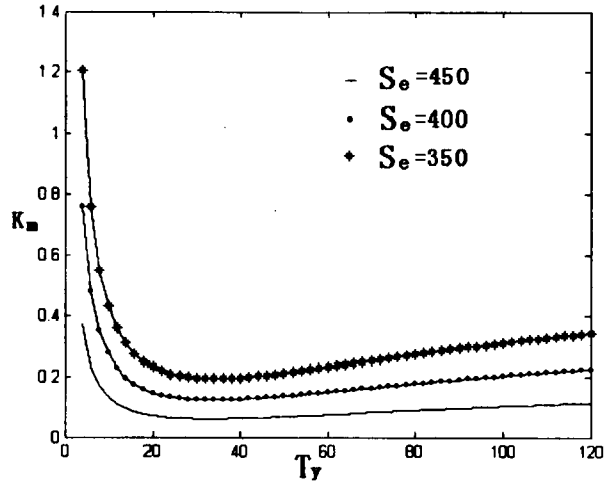

FIGURE 7. Relationship between K_m and yarn twist factor T_y.

TABLE I. Data of fiber properties used for calculation.

	Value	Unit
Fiber radius r_f	3×10^{-3}	cm
Fiber length l_f	3.0	cm
Fiber modulus E_f	6×10^7	g/cm^2
Fiber-fiber frictional efficient μ_1	0.3	–
Fiber-tension disk frictional coefficient μ_2	0.5	–
Fiber-grooved drum frictional coefficient μ_3	0.6	–
Fiber aspect ratio s	500	–
Whole compression W_t on the tension disk	5	g
Number of fibers in the yarn cross section n_1	100	–
Length of the tension disk L_g	4	cm

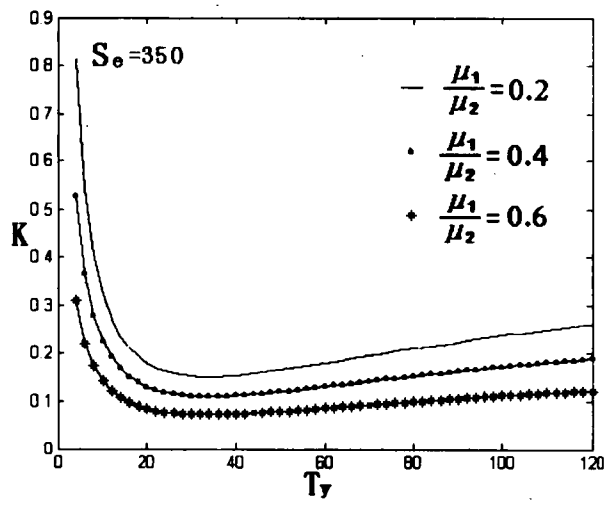

FIGURE 8. Relationship between K and T_y at different ratios of $\frac{\mu_1}{\mu_2}$.

thus the pullout force, increases with the twist factor. We also see from the figures that the values of both α_1 and α_2 are always positive.

In Equation 15, if the ratio $\frac{\mu_1}{\mu_2}$ tends to zero, K will reach its maximum value,

$$K_m = \frac{L_c}{f_1(T_y, S_e)(2L_c + L_{ave})} \quad , \qquad (17)$$

and its relations with both S_e and T_y are shown in Figure 7. In that figure, we see that only at the lowest $S_e = 350$ and $T_y < 10$ will K_m exceed 1. In other words, a fiber hair can be pulled out only when either the interfiber friction is much smaller than the fiber-tension disk friction, or the embedded fiber length is short (thus the low S_e), or the twist level is low. It seems that in general, fiber hairs can be pulled out, but with a certain difficulty as the yarn passes through the tension disk.

For a given S_e level, the effects of the ratio $\frac{\mu_1}{\mu_2}$ on the K value in Equation 15a are shown in Figure 8. We see that the value of K will decrease with the increasing ratio $\frac{\mu_1}{\mu_2}$ in the same T_y level; that is to say for a given interfiber friction μ_1, a reduction of fiber-tension disk friction μ_2 will decrease the impact on yarn hairiness by the tension disk during the winding process.

EFFECTS OF THE GROOVED DRUM

Although we have used the model in Figure 1 to study the fiber-tension disk interactions, it can also be used to analyze the effects of the grooved drum on yarn hairiness during the process, with following assumptions: First, the contacting width between the grooved drum and the cheese is similar to that in the tension disk contacting case, and second, the tension of the yarn is mainly

provided by the tension disk, so the tension in the yarn out of the contacting area is largely uninfluenced by the friction. As a result, when the tension in the yarn is T, Equation 14b can be modified to

$$P = T \cdot f_1(T_y, S_e) + \frac{T\mu_1}{R_c} \cdot f_2(T_y, S_e) \quad , \qquad (18)$$

where R_c is the radius of the cheese, which will increase with the winding process.

Equation 12b can be revised as

$$F_p = W_g \mu_3 \left(1 - \frac{\mu_1}{\mu_3} \frac{\tanh \beta}{\beta}\right) \quad , \qquad (19)$$

where μ_3 is the friction coefficient between the yarn and the grooved drum. W_g is the compression force between the grooved drum and the yarn on the cheese, so Equation 15a becomes

$$K = \frac{W_g \mu_3 \left(1 - \frac{\mu_1}{\mu_3} \frac{\tanh \beta}{\beta}\right)}{T \cdot f_1(q, S_e) + \frac{T\mu_1}{R_c} \cdot f_2(q, S_e)} \quad . \qquad (20a)$$

Here we define another nondimensional factor ϕ:

$$\phi = \frac{W_g \mu_3}{T} \quad . \qquad (20b)$$

During the whole winding process, the weight of the cheese increases with winding, and so do W_g and hence the dimensionless factor ϕ. Equation 20a cannot be solved directly due to the lack of a relation between the W_g and R_c. Here instead we define yet another parameter as

$$\xi = \frac{f_1(T_y, S_e)}{\frac{\mu_1}{R_c} \cdot f_2(T_y, S_e)} \quad . \qquad (20c)$$

From Equation 20c, we know the value of ζ will increase with R_c when the yarn structure is given. At different R_c values, the relation between ζ and the twist factor T_y is shown in Figure 9.

Figure 9 shows that the value of ζ becomes very large once the yarn twist factor is beyond a certain level. For instance, because the practical range for T_y is $38 - 80\left(\frac{\sqrt{\text{tex}}}{\text{cm}}\right)$ [22], the corresponding ζ value in the figure is 20 (when R_c = 5 cm) and 50 (when R_c = 10 cm). In other words, if we assume $\zeta \gg 1$ or $f_1(T_y, S_e) \gg \frac{\mu_1}{R_c} f_2(T_y, S_e)$, the maximum error is 1/20 or 5%, which seems acceptable.

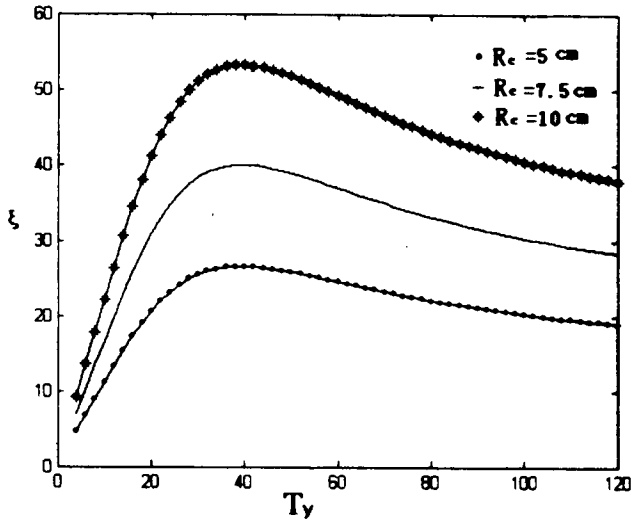

FIGURE 9. Value of ζ and the twist factor T_y.

Using the assumption above, Equation 20a can be rewritten as

$$K = \phi \frac{\left(1 - \frac{\mu_1}{\mu_3} \frac{\tanh \beta}{\beta}\right)}{f_1(T_y, S_e) + \frac{\mu_1}{R_c} \cdot f_2(T_y, S_e)}$$

$$\approx \phi \frac{\left(1 - \frac{\mu_1}{\mu_3} \frac{\tanh \beta}{\beta}\right)}{f_1(T_y, S_e)} \quad . \qquad (20d)$$

Again $\mu_3 > \mu_1$ is necessary, and $K > 1$ is both a necessary and sufficient condition for a protruding fiber being pulled out of the yarn.

During the winding process, μ_3 obviously remains constant, but the value of ϕ increases because of the growing cheese volume. From Equation 20d, for given yarn structure and winding conditions, K is determined explicitly by ϕ only. By setting the critical condition $K = 1$, the relation of the twist factor T_y and the critical value of ϕ at different embedded aspect ratios of hairiness S_e is obtained in Figure 10.

In Figure 10, the whole plane can be divided into two parts. If a point given by both twist factor T_y and ϕ falls in Part I where $K > 1$, the protruding fiber will be pulled out, while if the point is in Part II or $K < 1$, the fiber cannot be pulled out. From Figure 10, we can also observe that there exists an optimal twist level where the critical value of ϕ reaches its maximum, meaning that at this optimal twist level, the yarn gripping on all fibers is greatest, or the fibers are most likely not going to be pulled out. Deviating from this optimal twist level, the fibers become less resistant. Not surprisingly, this opti-

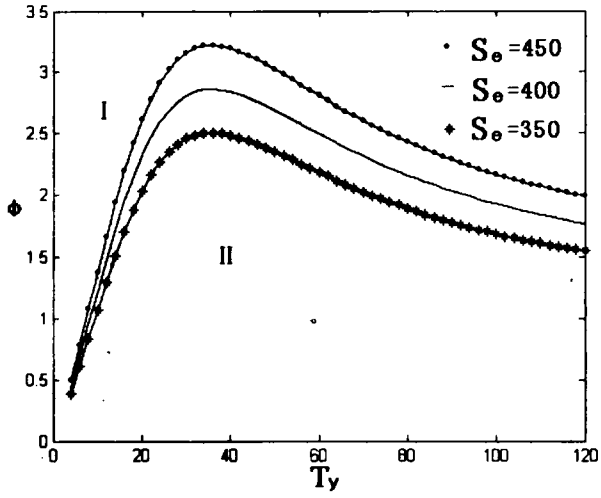

FIGURE 10. Relationship between ϕ and twist factor T_y at different S_e.

mal twist is likely the same as that leading to a maximum staple yarn strength; the decline is caused by the fiber obliquity effect.

Also from Figure 10, we see that the larger the S_e (thus the shorter the hair length), the greater the ϕ value at a given twist level, so the fiber is more difficult to pull out.

Conclusions

We have analyzed theoretically the impact of the winding process on yarn hairiness in this paper to provide a mathematical construct proving some previously known (through observation) concepts. First, for the effect of the tension disk, a criterion of whether such fiber pulling-out actually takes place is established by a ratio K of the total pulling out force to the gripping force exerted on the fiber during the winding process. Whereas by setting the ratio $K = 1$, the parameter ϕ can then be used as the criterion to study the influence of the grooved drum and cheese on yarn hairiness. More specifically, first, the effects of winding on yarn hairiness are determined by yarn structural characteristics such as the twist factor T_y and the embedded fiber length S_e and the winding conditions including the pressure W_t exerted on the yarn and the winding tension T. Second, for a given set of the other three parameters above, there is an optimal T_y level at which the yarn gripping force on the fibers reaches a maximum, just like yarn strength, making it most difficult for fibers to be pulled out. Third, understandably, increasing the yarn tension T, *i.e.*, winding speed V, or the embedded fiber length S_e or compression W_t will abate the impact on hairiness during winding. Fourth, the pulling-out criterion also depends on the relations between the frictional coefficients of interfiber μ_1, the fiber-tension disk μ_2, and the fiber-groove drum μ_3. Reducing either μ_2 or μ_3 will alleviate the impact on yarn hairiness during winding. Finally, when the yarn tension is constant, the value of ϕ can be reduced through decreasing compression between the grooved drum and the cheese so that the possibility of a fiber hair being pulled out drops off. This demonstrates that the method of adjusting the weight of the cheese to control the pressure between the cheese and the grooved drum is effective at alleviating the influence on yarn hairiness during the winding process.

Literature Cited

1. Barella, A., Yarn Hairiness: The Influence of Twist, *J. Textile Inst.* **48,** 268 (1957).
2. Carnaby, G. A., The Tensile Behavior of Staple Fiber Yarns at Small Extensions, *J. Textile Inst.* **67,** 299 (1976).
3. Chellamani, Yarn Quality Improvement with an Air-jet Attachment in Cone Winding, *Ind. J. Fiber Textile Res.* **25,** 289 (2000).
4. Datye, K. V., Minimizing Yarn Hairiness, *Ind. Textile J.* (8), 91 (1981).
5. Hearle, J. W. S., The Mechanics of Twisted Yarns: Tensile Properties of Continuous Filament Yarns, *J. Textile Inst.* **50,** T83 (1959).
6. Kilby, W. F., The Mechanical Properties of Twisted Continuous Filament Yarns, *J. Textile Inst.* **55,** T589 (1964).
7. Krishnaswamy, Influence of Winding on Hairiness, *BTRA Scan* **21,** 8 (1990).
8. Lridag, Y., The Influence of Testing Length and Speed on Yarn Hairiness, *Int. Textile Bull.* **3** (1999).
9. Morton, W. E., The Arrangement of Fibers in Single Yarns, *Textile Res. J.* **26,** 325 (1956).
10. Ozipek, B., Effects of Fiber Parameters on Yarn Hairiness, *Textile Month* (1), 29 (1999).
11. Pan, N., Development of a Constitutive Theory for Short Fiber Yarns: Mechanics of Staple Yarn Without Slippage Effect, *Textile Res. J.* **62,** 749 (1992).
12. Pan, N., Development of a Constitutive Theory for Short Fiber Yarns: Mechanics of Staple Yarn With Slippage Effect, *Textile Res. J.* **63,** 504 (1993).
13. Pan, N., Behavior of Yarn Pullout from Woven Fabrics: Theoretical and Experimental, *Textile Res. J.* **63,** 629 (1993).
14. Pan, N., Theoretical Modeling and Analysis of Fiber-pull-out Behavior from a Bonded Fibrous Matrix: The Elastic-bond Case, *J. Textile Inst.* **84,** 472 (1993).
15. Pan, N., A Modified Analysis of the Microstructural Characteristics of General Fiber Assemblies, *Textile Res. J.* **63,** 337 (1993).
16. Pan, N., Strengths of Twisted Blend Fibrous Structures: Theoretical Prediction of the Hybrid Effects, *J. Textile Inst.* **86,** 559 (1995).
17. Pan, N., Analytical Characterization of the Anisotropy and Local Heterogeneity of Short Fiber Composites: Fiber Fraction as a Variable, *J. Compos. Mater.* **28,** 1500 (1994).

18. Pillay, K. P. R., A Study of the Hairiness of Cotton Yarns, Part 1: Effect of Fiber and Yarn Factor, *Textile Res. J.* **34,** 663 (1964).
19. Platt, M. M., Mechanics of Elastic Performance Analysis of Textile Materials, Part III: Some Aspects of Stress Analysis of Textile Structures—Continuous Filament Yarns, *Textile Res. J.* **20,** 1 (1950).
20. Platt, M. M., Mechanics of Elastic Performance Analysis of Textile Materials, Part VI: Some Aspects of Stress Analysis of Textile Structures—Staple Fiber Yarns, *Textile Res. J.* **20,** 8 (1950).
21. Rust, J. P., Yarn Hairiness and the Process of Winding, *Textile Res. J.* **62,** 685 (1992).
22. Stanbury, G. R., WIRA, Leeds, England, 1949.
23. Tarafder, N., Effect of Post-Spinning Operation on the Hairiness of Ring Spun Cotton Yarn, *Ind. J. Fiber Textile Res.* **17,** 119 (1992).
24. Treloar, L. R. G., A Migrating-Filament Theory of Yarn Properties, *J. Textile Inst.* **56,** T359 (1966).
25. Wang, X., The Effect of Testing Speed on the Hairiness of Ring-spun and Sirospun Yarns, *J. Textile Inst.* **88,** 99 (1997).
26. Wang, X., Effect of Speed and Twist Level on the Hairiness of Worsted Yarns, *Textile Res. J.* **69,** 889 (1999).
27. Wang, X., A Study on the Formation of Yarn Hairiness, *J. Textile Inst.* **90,** 555 (1999).

Manuscript received July 22, 2003; accepted November 14, 2003.

Woven Fabric-Based Electrical Circuits

Part I: Evaluating Interconnect Methods

ANUJ DHAWAN, ABDELFATTAH M. SEYAM, TUSHAR K. GHOSH, AND JOHN F. MUTH[1]

College of Textiles, North Carolina State University, Raleigh, North Carolina 27695, U.S.A.

ABSTRACT

In recent years, a new area of research has emerged on textile-based electronics, called "electrotextiles." Most of the ongoing research in electrotextiles is driven by the motivation of creating multifunctional fiber assemblies that can sense, actuate, communicate, compute, etc. This paper discusses the development of fabric-based electrical circuits by interlacing conducting and nonconducting threads[2] into woven textile structures. Wired interconnections of different devices attached to the conducting elements of these circuits are made by arranging and weaving conductive threads so that they follow desired electrical circuit designs. In a woven electrically conductive network, routing of electrical signals is achieved by the formation of effective electrical interconnects and disconnects. Resistance welding is identified as one of the most effective means of producing crossover point interconnects and disconnects. Interconnects are evaluated by measuring the DC resistance associated with the crossover points of conducting threads.

The emerging field of electrotextiles can be viewed as an integration of technologies of materials, electronics, and textiles in order to create a new generation of flexible/conformable small or large multifunctional textile structures with electronic capabilities. These may include sensing and responding to environmental stimuli, energy generation to power "embedded" electronic devices, wired or wireless communication, etc. Fabric-based electrical circuits are fundamental to electrotextile products of the future. Woven fabrics, because of their structural order and ability to flex and conform to most desired shapes, offer an immediate opportunity to develop flexible electrical circuits. The current research on woven

[1] College of Engineering, North Carolina State University, Raleigh, NC.

[2] The term "conductive thread" in this context refers to conductive fibers, yarns, filaments, split films, etc., of metallic and/or polymeric materials.

  0040-5175/$15.00